Vietnam Journal of Catalysis and Adsorption
Tạp chí xúc tác và hấp phụ Việt Nam

Behavior of *n*-hexene-1 in hydroformylation of olefin mixtures over rhodium supported porous metal-organic framework MOF-5

Vu Van Toan[1,2*], Tong Thi Thanh Huong[1], Nguyen Thi Linh[1], Hendrik Kosslick[2,3], Axel Schulz[2,3]

[1] *Department of Oil Refining and Petrochemistry, Hanoi University of Mining and Geology, Duc Thang, Bac Tu Liem, Hanoi, VIETNAM.*
[2] *Institute for Catalysis, at the University of Rostock, Albert-Einstein-Str. 29a., D-18059 Rostock, GERMANY.*
[3] *Institute for Chemistry, the University of Rostock, Albert-Einstein-Str. 3a, D-18059 Rostock, GERMANY.*
Email: vuvantoan@humg.edu.vn; vutoan.humg@gmail.com

ARTICLE INFO

ABSTRACT

Metal organic framework MOF-5 was synthesized and used for the preparation of rhodium supported catalyst. Acetylacetonato(1,5-cyclooctadiene)rhodium(I) was used as catalyst precursor. The material was characterized by XRD, FTIR, TEM, AAS, and nitrogen adsorption. The catalytic properties of Rh@MOF-5 were investigated in the hydroformylation of olefins and olefin mixtures with different chain length to the corresponding aldehydes. High conversion and selectivity to *n*-aldehydes were achieved. Interestingly, shorter chain length molecule, *n*-hexene-1, shows different behavior in the hydroformylation of its mixtures, *n*-aldehyde is more favor in short reaction times. The obtained results indicate that rhodium active sites are highly dispersed inside the pores of the MOF-5 framework

1. Introduction

Porous MOFs are crystalline inorganic-organic hybrid materials, where metal clusters and organic ligands arranged in 3-dimensionaly interconnected forming porous crystalline frameworks. Metal sites and organic linkers are alternating periodically arranged and well separated. They possess a variety of properties such as high specific surface areas, tunable and extra-large pore sizes, and the possibility to functionalize, modify, or exchange organic linkers and metal compartments [1-3]. These outstanding features make them interesting as catalysts and supports for catalyst immobilization [4-6]. Therefore, the MOF materials have been attracted large attention [7-9].

Hydroformylation of olefins is one of the most important homogeneous catalyzed reactions in fine chemistry [10, 11]. Hydroformylation reaction was

discovered by Otto Roelen in 1938 [12]. It is the reaction of the olefinic double bonds with the mixture of hydrogen and carbon monoxide (synthesis gas) yielding to linear and branched aldehydes as primary products. Additionally, double bond shifted *i*-alkene is also formed as follows.
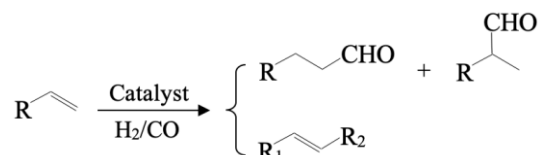
The linear aldehydes are valuables used for production of alcohols, which are important chemical intermediates [13]. About more than 10 million tons of aldehydes and alcohols are manufacturing a year by the hydroformylation [14]. These products find applications in the production of plasticizers, detergents, adhesives and solvents [15, 16] The

branched aldehydes are less favored products; however, they can be used in the synthesis pharmaceuticals and agrochemicals, especially if they contain a chiral carbon atom [13]. Both cobalt and rhodium based homogeneous catalysts are used in the industrial hydroformylation process. Although homogeneous catalysts give high conversion and selectivity for desired product in shorter reaction time as heterogeneous catalyst systems, separation of homogeneous catalysts from product mixture is a challenge [17, 18]. Therefore, heterogenization of homogeneous catalysts is still of interest. Several support materials including MCM-41, silica, alumina, zeolites, activated carbons, polymeric organic, inorganic and hybrid supports, supported aqueous phase catalysis (SAPC) have been studied [19, 20]. Main disadvantages of these supported catalysts are leaching of rhodium complex during the reaction, complicated synthesis procedure, lower catalyst activity, selectivity and thermal instability [17].

Application of metal-organic frameworks as catalyst supports in the hydroformylation reaction have been reported [4, 21-23]. The exceptional characteristics allow MOFs potentially employing in this type of reaction under mild conditions. In this work, the MOF-5 support materials were prepared and tested in the hydroformylation of linear n-alkenes with different chain length. Furthermore, mixtures of olefin reactants were also employed in the hydroformylation to investigate the influence of the structure of the porous MOF frameworks in this reaction.

2. Experimental Section

Materials

Synthesis of MOF-5

MOF-5 was synthesized by optimized procedures referred to literature [7-9, 24]. Zn(NO3)$_2$ (zinc nitrate), H$_2$BDC (terephthalic acid) and DMF (dimethylformamide) were used as starting materials and solvent.

In a typical procedure, 0.332 g of H$_2$BDC (Merck) and 1.569 g of Zn(NO3)$_2$·4H$_2$O (Merck) were dissolved in 50 mL of DMF (Merck). The solution was given into a glass reactor which was equipped with a drying tube on overhead end. The mixture was heated to 105 °C under stirring. Then the mixture was allowed to crystallize at 105 °C for 24 h under static condition. Thereafter, the glass reactor was cooled down naturally to room temperature.

The crystallized product was filtered off and washed three times with 10 mL of CH$_2$Cl$_2$. The recovered solid was suspended in 50 mL of DEF and heated under stirring at 130 °C for 1 h. Then the solid was filtered off and washed 3 times with 10 mL of CH$_2$Cl$_2$. Next, it was given into 50 mL of CH$_2$Cl$_2$ and stirred for 12 h at room temperature. Then the solid was again filtered off and washed three times with 10 mL of CH$_2$Cl$_2$. Finally, the solid product was dried under vacuum condition at 105 °C for 12 h to obtain an as-synthesized MOF-5.

Rhodium loading

The procedure of rhodium loading on the MOF-5 support was carried out under argon atmosphere. Typically, 10 mg of Rh(acac)(cod) [(acetylacetonato)(cycloocta-1,5- diene)rhodium(I)] was poured into a beaker glass containing 28 mL of acetonitrile (Baker) and 20 mL of toluene (Merck) under stirring. A clear pale-yellow solution was formed. Then 4 g of the as-synthesized MOF-5 was added under mild stirring. The suspension was slowly heated to $ca.$ 70 °C to evaporate the solvent. The obtained product was washed three times with 5 mL of toluene and dried at 70 °C under vacuum. The resulting Rh@MOF-5 catalyst was used for catalytic testing.

Characterization

The MOF-5 and Rh@MOF-5 were characterized in detail by XRD, FTIR, TEM, AAS, and nitrogen sorption measurements. The XRD measurements were carried out on the STADI-P (STOE) X-ray diffractometer using using Ni-filtered CuKα radiation (λ = 1.5418 Å). IR spectroscopic measurements were performed on a Nicolet 380 FTIR spectrometer coupled with smart orbit ATR device with a resolution of 4 cm^{-1}.

Textural properties were studied by TEM and nitrogen sorption measurements. TEM measurements were carried out with a LIBRA 120 electron microscope (Carl Zeiss, Oberkochen) at 120 kV with a resolution of 0.35 nm. Images were recorded with a digital camera with 2000 x 2000 pixels. Nitrogen adsorption measurements were performed on an ASAP 2010 sorption system. Before measurements, the samples were dried by heating at 150 °C under reduced pressure. The measurements were carried out at -196 °C. The rhodium content was determined by atomic absorption spectrometry with an AAS-Analyst 300 device (Perkin Elmer). A nitrous oxide/acetylene or air/acetylene mixture was used for the burner system.

Catalytic testing

Olefins with different chain length as *n*-hexene-1 (≥ 97 %, Aldrich), *n*-octene-1 (≥ 98 %, Aldrich), *n*-decene-1 (≥ 95 %, Acros) and *n*-dodecene-1 (93-95 %, Acros) were used for the olefin hydroformylation reactions catalyzed by the Rh@MOF-5 catalyst. In single component reactions, one olefin as *n*-hexene-1, *n*-octene-1, *n*-decene-1 or *n*-dodecene-1 was used. Additionally, mixtures of two olefin components were also employed in the reaction. The catalytic activity of the parent MOF-5 alone (without rhodium) has been checked in a blank experiment. All hydroformylation experiments were carried out in a 100 mL PARR reactor at 100 °C and 50 bar (CO/H_2 = 1) under stirring at *ca.* 1000 rpm. Toluene was used as solvent.

Typically, for the *n*-hexene-1 hydroformylation, 95 mg of Rh@MOF-5, 12.5 mL of *n*-hexene-1, and 30 mL of toluene were loaded into the reactor. The *n*-hexene-1 to catalyst molar ratio based on rhodium was *ca.* 100,000/1. After loading, the reactor was evacuated and purged with argon. The procedure was repeated in order to remove air and residual moisture. Thereafter, the reactor was immediately loaded with synthesis gas up to a pressure of 50 bar at room temperature. Finally, the reaction mixture was heated under stirring at *ca.* 1000 rpm and maintained at a temperature of 100 °C during the course of reaction. The reactor was equipped with a gas introduction stirrer. The reactions of other olefins and olefin mixtures were carried out in the same way. The molar olefin/Rh ratio was kept constant.

3. Results and discussion

Materials

The crystallinity and structural origin of as-synthesized MOF-5 and Rh loaded form Rh@MOF-5 were checked by powder X-ray diffraction.
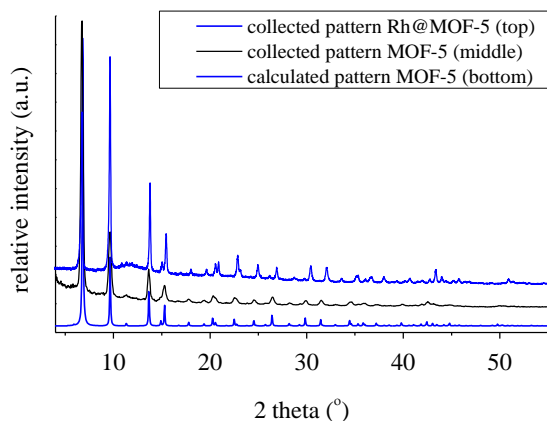

Fig. 1. XRD pattern of MOF-5 and Rh@MOF-5.

As shown in Fig. 1, the reflections are well resolved. The similarity of XRD patterns obtained with as-synthesized MOF-5 and Rh loaded form Rh@MOF-5 indicates that the structure of MOF framework is maintained after Rh loading. The collected patterns are in accordance with the calculated pattern and also in agreement with previously reported patterns of MOF-5 [3, 25].

TEM images of MOF-5 are shown in Fig. 2 (a, b). It is clear that MOF-5 consists of well crystalized elongated nanocrystals. They are uniform with the dimensions of *ca.* 70 x 200 – 250 nm.
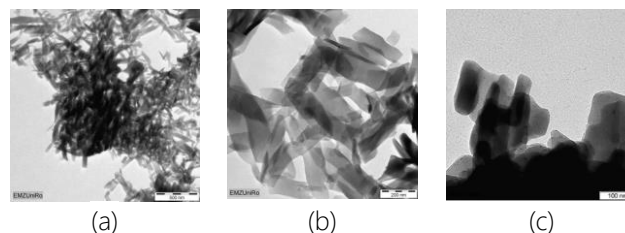

Fig. 2. TEM images of (a) and (b) as-synthesized MOF-5 and (c) Rh@MOF-5.

The nanocrystals tend to agglomerate and are in part intergrown. The presence of intracrystalline nanoporosity has not been detected by TEM. No rhodium particle was found in TEM image, Fig. 2 (c). This proves that high dispersion of rhodium sites has been achieved in the prepared Rh@MOF catalyst sample.

FTIR spectra of as-synthesized MOF-5 and the Rh@MOF-5 supported catalyst in the spectral range of 500 – 2500 cm^{-1} are shown in Fig. 3 (a). They are well resolved and show the typical vibration bands observed of benzene carboxylate group, which is present as a linker. The spectra are dominated by strong absorbances between about 1350 – 1600 and 740 – 825 cm^{-1}. These bands are related to vibration modes of carboxylate groups and different =C–H modes of the phenyl groups.

The high frequency vibration band of carboxylate group COO^- is located at 1602.8 cm^{-1}, Fig. 3 (a). It is distinctly lower than the frequency of the corresponding absorption bands of the protonated carboxyl group - COOH - which appears at 1760 – 1690 cm^{-1}. This finding indicates deprotonation of 1,4-benzenedicarboxylate linker in the framework of MOF-5 upon the reaction with Zn metal ions [26].

Markedly low frequency shifts (*ca.* 20 cm^{-1}) and in part vibration band splitting are observed after rhodium loading. For instances, the peak at: 1602.8 cm^{-1} is shifted to 1574.3 cm^{-1}, 1506.3 cm^{-1} to 1500.3 cm^{-1}, 1392.0 cm^{-1} to 1371.7 cm^{-1}, 1018.5 cm^{-1} to 1015.4 cm^{-1}, 823.9 cm^{-1} to 808.9 cm^{-1}, and 576.3 cm^{-1} to 548.9 cm^{-1},

respectively. Such low frequency shifts are usually found with strong interacting metal ions. It confirms that the rhodium site is most probably located inside the pores of the MOF-5 framework [21]. Based on AAS analysis, the rhodium content in the Rh@MOF-5 catalyst is 0.145 %. On average, the framework contains only one rhodium atom per three hundred benzene dicarboxylate linkers. Nevertheless, severe shifts of linker modes are observed in the IR spectrum. This additionally confirms the strong interactions between rhodium and the organic linker as well as the high dispersion of rhodium sites in the MOF framework.
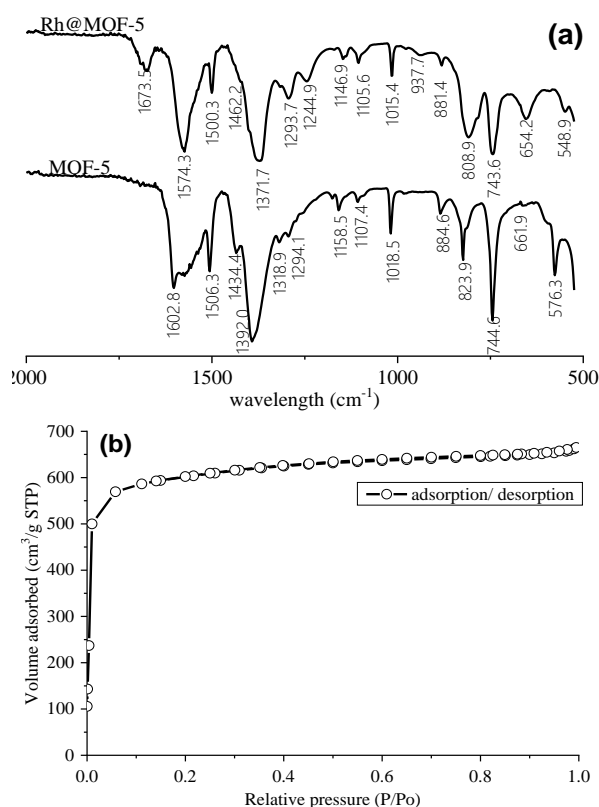

Fig. 3. FTIR spectra of as-synthesized MOF-5 and Rh-loaded form Rh@MOF-5 (a); and Nitrogen adsorption/ desorption isotherm of as-synthesized MOF-5 (b).

The specific surface area and pore volume of as-synthesized MOF-5 was investigated by nitrogen adsorption measurements. A typical nitrogen adsorption/ desorption isotherm obtained with MOF-5 is shown in the Fig. 3 (b). It belongs to type I according to the IUPAC nomenclature [27]. At very low relative pressure, strong nitrogen uptake indicated by the steep of the isotherm is due to adsorption in the micropores of the MOF-5 framework. There is only a slightly increase of the nitrogen uptake up to a relative pressure $ca.$ P/P$_0$ = 0.5 because of adsorption in small mesopores having diameters of 2 – 5 nm. However, the TEM image shows no intraparticle mesoporosity.

Hence, these pores are due to textural porosity between the MOF nanoparticles. The BET surface area of MOF-5 is of 2300 m^2/g and pore volume of 1.0 cm^3/g. The high surface area and pore volume might enable reactant to access to rhodium active sites proposedly located in the pore system of the MOF-5 framework.

Catalysis

The catalytic performance of the supported Rh@MOF-5 catalyst was investigated using hydroformylation of n-alkene-1 with different chain lengths. The results show that hydroformylation of n-alkenes resulted in the formation of n- and i-aldehydes as well as of double bond shifted i-alkenes. The double bond shift reaction is catalyzed by acid sites of MOF-5. They might be connected with the metal sites.

Reaction of single olefin component

The total conversions of different terminal alkenes as n-hexene-1 (C$_6$), n-octene-1 (C$_8$), n-decene-1 (C$_{10}$), and n-dodecene-1 (C$_{12}$) to aldehydes and internal (i-) alkenes in the hydroformylation are shown in Fig. 4 (a). As revealed, the total conversion almost linearly increases with reaction time during 0 – 5 h of reaction. The conversion of the longer chain molecule C$_{12}$ is lower compared to shorter chain ones. This indicates that the catalytic reaction takes place mainly inside the pores of the MOF-5 framework. After 1 h of reaction, the total conversions are already $ca.$ 40 % with C$_8$ and C$_{10}$ compared to only 13 % with C$_{12}$. Interestingly, the shorter one C$_6$ proceeds significantly slower than that of longer chains C$_8$ and C$_{10}$. It is only 15% after 1h of reaction. However, it proceeds faster afterward, during 1 – 3 h of reaction. Except for C$_{12}$, total conversions of nearly 100% are already achieved after 4 – 5 h of reaction.

The selectivities to aldehydes are nearly unchanged during 1 – 5 h of reaction and vary between 25% and 30% depending on substrates, Fig. 4 (b). They further increase after prolonged reaction time, 21 h, due to the hydroformylation of double bond shifted i-alkenes to the corresponding aldehydes.

The conversion of the i-alkenes to the corresponding i-aldehydes with prolonged reaction time is also reflected in n/i-aldehyde ratio, Fig. 4 (c). In the first 3 h of reaction, n/i-ratios vary in between 3.4 – 3. However, they decrease fast afterward, especially with C$_8$ and C$_{10}$ which are already achieved nearly maximum conversion after only 4 h of reaction, Fig. 4 (a). With the prolonged reaction time, the low n/i-aldehyde ratios are due to the accumulation of i-aldehydes converted from the aforesaid corresponding i-olefins previously created in the reaction mixture and also due

to aldol condensation which compensate the *n*-aldehyde product to form bigger aldehydes. This reaction has been observed in the hydroformylation of olefins catalyzed by Rh@MIL-101 [21]. As a result, the *n/i*-ratios of only 0.8 – 0.9 and 1.6 for dodecene-1 were achieved after 21 h of reaction, Fig. 4 (c).
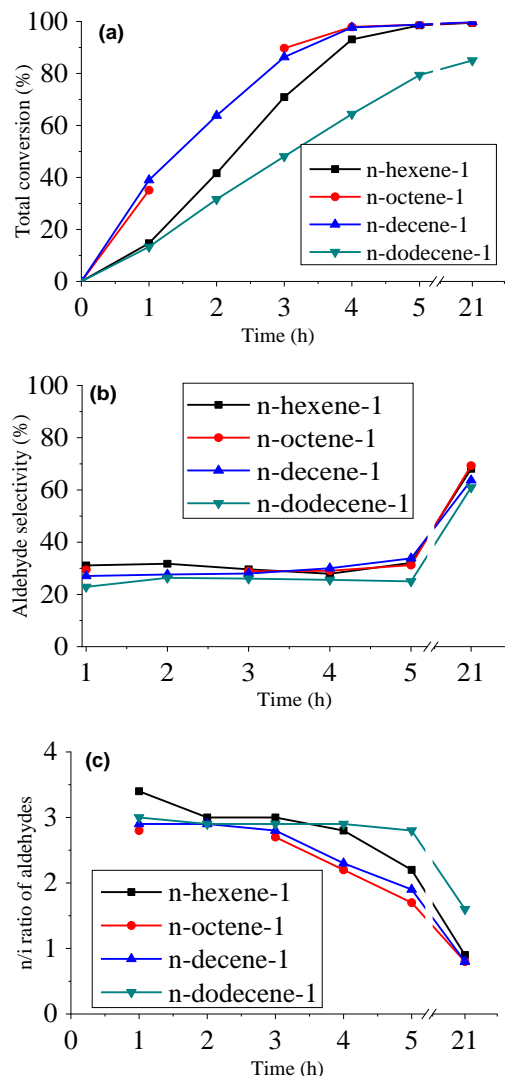

Fig. 4. Total conversion, aldehyde selectivity, and *n/i*-aldehyde ratio in the hydroformylation of single *n*-alkene-1 over Rh@MOF-5 catalyst.

Reaction of olefin mixture

The results of hydroformylation of *n*-hexene-1 (50%) and *n*-octene-1 (50%) mixture over Rh@MOF-5 are shown in Fig. 5 (a, b). As shown, both two components in the mixture are rapidly converted. They proceed significantly faster compared to that of single component reaction (Fig. 4). Nearly 100% of both C_6 and C_8 are converted to aldehydes and internal olefins just after 3 h of reaction compared to only 71 – 90% in cases of single olefin reactions (Fig. 4a). As a result, the

aldehyde selectivities for both C_6 and C_8 gradually increase, especially from 3-5 h of reaction, Fig. 5 (b). In case of the single component reaction, the aldehyde selectivities seem to be constant from 1 – 5 h of reaction.
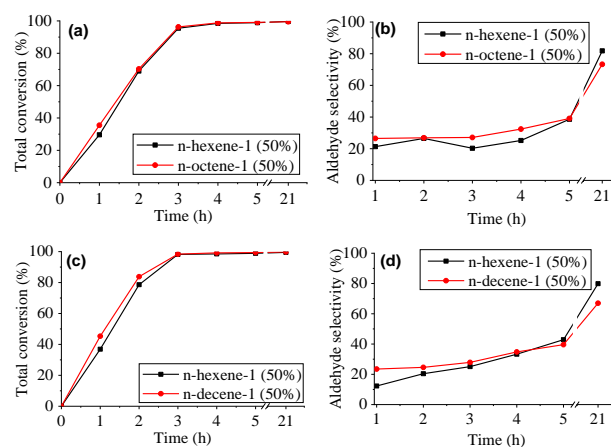

Fig. 5. Total conversion and aldehyde selectivity in the hydroformylation of mixture 1 of C_6 and C_8 (a, b) as well as mixture 2 of C_6 and C_{10} (c, d) over Rh@MOF-5 catalyst.

The *n/i*-aldehyde ratios are shown in Tab. 1. In case of C_8, the ratio decreases very fast compared to that of its single component reaction. It is because, with C_8, higher conversion is already achieved after short reaction time. An increasing reaction time of more than 3 h is for the conversion of *i*-olefins to corresponding aldehydes. It is therefore more *i*-aldehydes are achieved whereas there is no further *n*-aldehyde created. As a result, the *n/i*-ratio significantly decreases. However, it is observed that the *n/i*-ratio for C_6 is extremely exceptional as shown in Tab. 1 (mixture 1). After 1 h of reaction, the ratio is up to 13.2. For other reaction times, the ratio is still very high. These abnormal results have never been detected in any single component reactions.

Table 1. *n/i*-Aldehyde ratio in the hydroformylation of mixture 1 of C_6 and C_8 and mixture 2 of C_6 and C_{10} over Rh@MOF-5 catalyst.

Reaction time (h)	*n/i*-Aldehyde ratio in reaction of mixture 1		*n/i*-Aldehyde ratio reaction of mixture 2	
	C_6	C_8	C_6	C_{10}
1	13.2	2.9	13	2.8
2	3.2	2.8	6.3	2.7
3	4.6	2.4	3.7	2.1
4	3.8	1.8	1.8	1.5
5	1.8	1.4	1.4	1.3
21	0.8	0.7	0.8	0.7

Similar to the behavior shown with the reaction mixture 1 of *n*-hexene-1 and *n*-octene-1, the results with the reaction mixture 2 of *n*-hexene-1 and *n*-decene-1 are revealed in Fig. 5 (c, d). As presented, both components proceed very fast and reach nearly 100% after 3 h of reaction. As a result, the aldehyde selectivities are high and the aldehyde yields constantly increase during 1 – 5 h of reaction accordingly.

With C_{10}, the *n/i*-aldehyde ratio continuously decreases during 1-5 h of reaction and goes down to 0.7 after 21 h of reaction, Tab. 1, (mixture 2). This decrease is faster compared to that of single component reaction also due to the accumulation of *i*-aldehydes converted from corresponding *i*-alkenes. Like the reaction of C_6 and C_8 mixture, extremely high *n/i*-ratios are also achieved with C_6 at 1, 2, and 3 h of reaction. This can be explained by the advanced competence of the shorter chain C_6 molecule in comparison with other longer chain molecules in reaction mixture with highly possibility for its double bond head arranged to Rh active sites in the pores of the MOF framework. For the longer chain molecules like C_8, C_{10} in reactant mixtures, this arrangement would be more difficult. It is quite different in case of single component reactions of C_6 in which the competency in between reactants are the same. No priority is accepted, all the same components compete each other, it is therefore, less double bond heads of C_6 molecules would go inside the pores of the MOF framework. As a result, less *n*-aldehydes of C_6 could be achieved in this case. These interesting results also indicate that the rhodium active sites are located inside the pores of the MOF structure. This finding is in agreement with the strong interactions between rhodium sites and the MOF structure indicated by FTIR vibration band shifts after rhodium loading on the MOF.

4. Conclusion

Well crystallized metal-organic framework MOF-5 was synthesized and used for the preparation of rhodium supported Rh@MOF-5 catalyst. The catalytic performance was studied in the hydroformylation of different chain length terminal *n*-alkenes to aldehydes. Despite low Rh loading, the catalyst is highly active which is appointed to the high dispersion of rhodium active sites in the inorganic organic hybrid framework. The catalyst is very selective compared to other supports like MCM-41, SBA-15. The *n/i*-aldehyde ratios normally reach up to 3 in all reactions. The coordinatively unsaturated metal sites in the MOF framework and rhodium species could accelerate

double bond shift reaction to form internal alkenes leading to high values of *i*-aldehydes after long time of reaction. *n*-Hexene-1 shows interesting behavior in the hydroformylation of its mixtures because of its superior competence with its shorter chain length compared to the others in the reaction mixtures. However, it should be further studied over diffent MOF supports to figure out the importance of the framework of MOF to the hydroformylation reaction.

Acknowledgments

References

1. G. Férey, C. Mellot-Draznieks, C. Serre, F. Millange, J. Dutour, S. Surblé, I. Margiolaki, Science 309 (2005) 2040-2042. https://doi.org/10.1126/science.1116275
2. S. Hermes, M.K. Schroter, R. Schmid, L. Khodeir, M. Muhler, A. Tissler, R.W. Fischer, R.A. Fischer, Angew. Chem. Int. Ed. 44 (2005) 6237-6241. https://doi.org/10.1002/anie.200462515
3. O.M. Yaghi, M. O'Keeffe, N.W. Ockwig, H.K. Chae, M. Eddaoudi, J. Kim, Nature 423 (2003) 705-714. https://doi.org/10.1038/nature01650
4. T.V. Vu, H. Kosslick, A. Schulz, J. Harloff, E. Paetzold, J. Radnik, U. Kragl, G. Fulda, C. Janiak, N.D. Tuyen, Micropor. Mesopor. Mater. 177 (2013) 135-142. https://doi.org/10.1016/j.micromeso.2013.02.035
5. Y. Du, X. Jia, L. Zhong, Y. Jiao, Z. Zhang, Z. Wang, Y. Feng, M. Bilal, J. Cui, S. Jia, Coord. Chem. Rev. (2021) 214327. https://doi.org/10.1016/j.ccr.2021.214327
6. K.-G. Liu, Z. Sharifzadeh, F. Rouhani, M. Ghorbanloo, A. Morsali, Coord. Chem. Rev. 436 (2021) 213827. https://doi.org/10.1016/j.ccr.2021.213827
7. U. Mueller, M. Schubert, F. Teich, H. Puetter, K. Schierle-Arndt, J. Pastre, J. Mater. Chem. 16 (2006) 626-636. http://dx.doi.org/10.1039/B511962F
8. S. Hermes, F. Schroder, S. Amirjalayer, R. Schmid, R.A. Fischer, J. Mater. Chem. 16 (2006) 2464-2472. https://doi.org/10.1039/B603664c
9. H. Li, M. Eddaoudi, M. O'Keeffe, O.M. Yaghi, Nature 402 (1999) 276-279. https://www.nature.com/articles/46248
10. P.C.J. Kamer, J.N.H. Reek, P.W.N.M. van Leeuwen, in: B. Heaton (Ed.), Mechanisms in Homogeneous Catalysis, A spectroscopic Approach, Wiley-VCH, Weinheim, 2005, p. 231. https://doi.org/10.1021/ja0597956
11. M. Marchetti, S. Paganelli, E. Viel, J. Mol. Catal. A Chem. 222 (2004) 143-151. https://doi.org/10.1016/j.molcata.2004.07.022
12. B. Cornils, W.A. Herrmann, M. Rasch, Angew. Chem. Int. Ed. 33 (1994) 2144-2163. https://doi.org/10.1002/anie.199421441

13. S. Bektesevic, A.M. Kleman, A.E. Marteel-Parrish, M.A. Abraham, J. Supercrit. Fluids 38 (2006) 232-241. http://dx.doi.org/10.1016/j.supflu.2006.01.019

14. A. Boerner, R. Franke, Hydroformylation: Fundamentals, Processes, and Applications in Organic Synthesis, Wiley-VCH, 2016, p. 1.

15. C.D. Frohning, C.W. Kohlpaintner, Applied Homogeneous Catalytic with Organometallic Compounds 2ed., Wiley-VCH, 2003, p. 31.

16. H.-W. Bohnen, B. Cornils, Advances in Catalysis, Academic Press, 2002, pp. 1-64.

17. S.K. Sharma, P.A. Parikh, R.V. Jasra, J. Mol. Catal. A Chem. 316 (2010) 153-162. https://doi.org/10.1016/j.molcata.2009.10.014

18. M.S. Shaharun, B.K. Dutta, H. Mukhtar, S. Maitra, Chem. Eng. Sci. 65 (2010) 273-281. https://doi.org/10.1016/j.ces.2009.06.071

19. C.O. Oseghale, B.M. Mogudi, C.A. Akinnawo, R. Meijboom, Appl. Catal. A Gen. 602 (2020) 117735. https://doi.org/10.1016/j.apcata.2020.117735

20. J.A. Bae, K.-C. Song, J.-K. Jeon, Y.S. Ko, Y.-K. Park, J.-H. Yim, Micropor. Mesopor. Mater. 123 (2009) 289-297. https://doi.org/10.1016/j.micromeso.2009.04.015

21. T. Van Vu, H. Kosslick, A. Schulz, J. Harloff, E. Paetzold, M. Schneider, J. Radnik, N. Steinfeldt, G. Fulda, U. Kragl, Appl. Catal. A Gen. 468 (2013) 410-417. http://dx.doi.org/10.1016/j.apcata.2013.09.011

22. D. Gorbunov, M. Nenasheva, E. Naranov, A. Maximov, E. Rosenberg, E. Karakhanov, Appl. Catal. A Gen. 623 (2021) 118266. https://doi.org/10.1016/j.apcata.2021.118266

23. Y. Sun, J. Harloff, H. Kosslick, A. Schulz, C. Fischer, S. Bartling, M. Frank, A. Springer, Mol. Catal. (2021) 112005. https://doi.org/10.1016/j.mcat.2021.112005

24. S.S. Kaye, A. Dailly, O.M. Yaghi, J.R. Long, J. Am. Chem. Soc. 129 (2007) 14176-14177. https://doi.org/10.1021/ja076877g

25. D. Britt, D. Tranchemontagne, O.M. Yaghi, Proc. Natl. Acad. Sci. U.S.A 105 (2008) 11623-11627. https://doi.org/10.1073/pnas.0804900105

26. N.T.S. Phan, K.K.A. Le, T.D. Phan, Appl. Catal. A Gen. 382 (2010) 246-253. https://doi.org/10.1016/j.apcata.2010.04.053

27. R.S. Mikhail, E. Robens, Microstructure and thermal analysis of solid surfaces, John Wiley & Sons Limited, Chichester, 1983.